Electron capture from a metal surface by slow, multicharged aluminum and carbon ions

R. H. Hughes, R. D. Miller, G. Wattuhewa, X. M. Ye,* and D. O. Pederson
Department of Physics, University of Arkansas, Fayetteville, Arkansas 72701
(Received 23 February 1989)

A time-of-flight technique has been used to measure residual charge in the scattering of laser-produced pulses of C^{k+} ($k=1$ to 4) and Al^{m+} ($m=2$ to 5) ions from a well-outgassed amorphous gold-iridium surface under UHV conditions (2×10^{-9} Torr). Ions incident at 7° to the surface were specularly reflected. The analysis showed the survival of singly charged ions in the case of scattering 300-, 400-, and 500-eV/charge Al ions with neutrals representing the majority species. This is equivalent to a kinetic energy in a direction transverse to the surface of 4.5, 5.9, and 7.4 eV/charge, respectively, which ensures only minimal surface penetration. In the case of 280-eV/charge carbon ions, only neutrals were detected. No residual ions were detected in either Al or C ions scattered through an angle of deviation equal to or greater than 45° within experimental error. In a separate experiment no residual ions were detected in the case of 400-eV/charge Al ions incident at 22.5° to a gold surface and specularly reflected. The results are explained in terms of Auger neutralization of the multicharged ions on the incoming pass and resonance ionization and neutralization of low-charge-state ions that emerge from the surface and change their charge on the outgoing pass. Under near adiabatic conditions, no residual charge is expected for either the aluminum or carbon projectiles. The presence of Al^+ under grazing-incidence and specular reflection is analyzed and discussed in terms of the nonadiabatic behavior of Al^+ ions emerging from the surface.

INTRODUCTION

In a previous publication[1] we reported the survival of only singly charged aluminum ions when slow (near 400 eV per charge) multicharged aluminum ions (Al^{m+} where $m=2$ to 6), incident at 7° to a gold surface, were specularly reflected. It was suggested that the ion-neutral fractions did not appear to be a strong function of the incident charge state and was consistent with a model in which the highly charged incident ions are rapidly Auger neutralized in a step-wise fashion[2] to Al^+ with neutralization completed by resonance neutralization since the ground state of Al^0 is 6.0 eV, which is below the Fermi level of gold. Since that preliminary report the apparatus has been improved and we now can report more quantitative results.

APPARATUS

Figure 1 shows our apparatus. The ion source is a laser ion source.[3] The laser has been upgraded in power since the works described in Ref. 3 were done. This upgraded source was used in Ref. 1 and was used in the study of the end-point energies of Auger-ejected electrons when multicharged ions are near a gold surface.[4] The ions are produced by 15-ns 800-mJ bursts of neodymium-doped yttrium aluminum garnet (Nd:YAG) laser light focused onto a solid target. The resulting plasma plume advances toward the entrance of a 180° electrostatic analyzer where ion packets with a particular energy per charge are selected. The ion packets travel through a deceleration-acceleration einzel lens ($L1$), ion gate (IG), and acceleration-deceleration einzel lens ($L2$) to the collision chamber where the gold-iridium ion target is housed. Scattering from the target takes place near grazing incidence at about 7° to the surface. The ion packets then are specularly reflected down the long charge analysis arm. The scattered packets pass through a screened retarding gap (RG) where the charged component is slowed and allowed to drift in an equipotential environment provided by a positively charged drift tube (DT). The ions pass through an exit screen and are accelerated back to ground potential. The ions impact onto a Galileo Chevron (channel plate) detector ($C1$) which we will refer to as a CEMA to be consistent with Ref. 4. The charge separation is thus done through a time-of-flight technique (TOF) where the neutral component of the scattered packet arrives in time before the ionic component.

The ion drift region is surrounded by a strong longitudinal magnetic field provided by magnetic coils (MC's). The magnetic field is necessary to prevent ion loss due to space-charge repulsion effects. The CEMA detection efficiency is not affected by the magnetic field because the pore size of the channel plate is much smaller than the Larmor radius of the secondary electrons induced in CEMA.

The CEMA detector is operated in this study with the front end at ground potential. This insures that for each ion packet that is scattered from the gold-iridium target the neutral component and the surviving Al^+ component will each strike the CEMA at the same velocity. Since the first ionization potential for aluminum is only 6.0 eV, appreciable secondary electron production in the CEMA by potential ejection is not expected, and thus secondary electron production in the CEMA is essentially all due to kinetic ejection. Operating the CEMA front end at ground potential allows us to detect the neutral com-

ponent and the Al^+ component in each scattered packet with identical detection efficiency.

Not shown in Fig. 1 is a 250-W heater system that can radiantly heat the ion target and provide the source of a 6-W electron beam which can bathe the target with 3-kV electrons. The target used in this study was subjected to a 200° C bakeout with the entire vacuum system, plus an extended period under the electron beam bath. The base pressure extended into the 10^{-10} Torr region with chamber pressure rising to near 2×10^{-9} Torr during operation of the laser ion source.

The ion target was nominally a first surface gold mirror with no overcoat. The mirror consists of an iridium coated glass plate overcoated with gold. The target was subjected to severe outgassing with the electron gun assembly. The treatment resulted in amalgamating the iridium with the gold producing a mirror with the physical appearance of gold but without evidence of the iridium substrate.

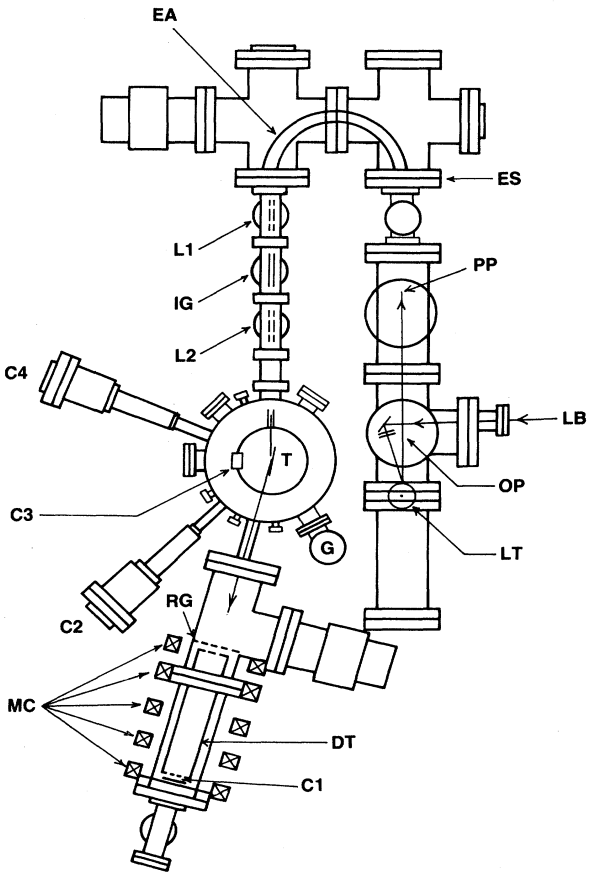

FIG. 1. Schematic diagram of the apparatus. LB, laser beam; OP, vacuum optics; LT, laser target; PP, plasma plume; ES, electron stripping screen; EA, 180° electrostatic analyzer; *L*1, deceleration-acceleration-einzel lens; IG, ion gate; *L*2, acceleration-deceleration-einzel lens; *T*, gold-iridium target; RG, ion retarding gap; DT, ion drift tube; *C*1, CEMA particle detector; MC, magnetic coils for ion collection; *G*, residual gas analyzer. *C*2, *C*3, and *C*4 are CEMA particle detectors used in other scattering diagnostics.

RESULTS

Figure 2 shows the results of about 400-eV/charge aluminum 2+, 3+, and 4+ ions scattered from a gold surface at three different retarding potentials. Note that the 800-eV Al^+ ions from the 2+ packet are completely stopped in Fig. 2(c).

In Fig. 3, we show plots representative of the charge separation technique in the scattering of about 2000-eV 5+, 1600-eV 4+, 1200-eV 3+, and 800-eV 2+ ion packets. The ion packet plots shown in Fig. 3 are obtained by gating the packets so that only the wanted packet is allowed through the IG shown in Fig. 1. This proves very useful in that measurements can be made on a given charge packet without interference from an adjacent charge packet.

The relative amount of singly charged ions left in a packet after scattering is determined by measuring the relative areas under the Al^0 and Al^+ envelopes such as in Fig. 3.

Attempts were made to determine the charge fraction left when slow carbon ions (C^{n+}, $n=1$ to 4) were scat-

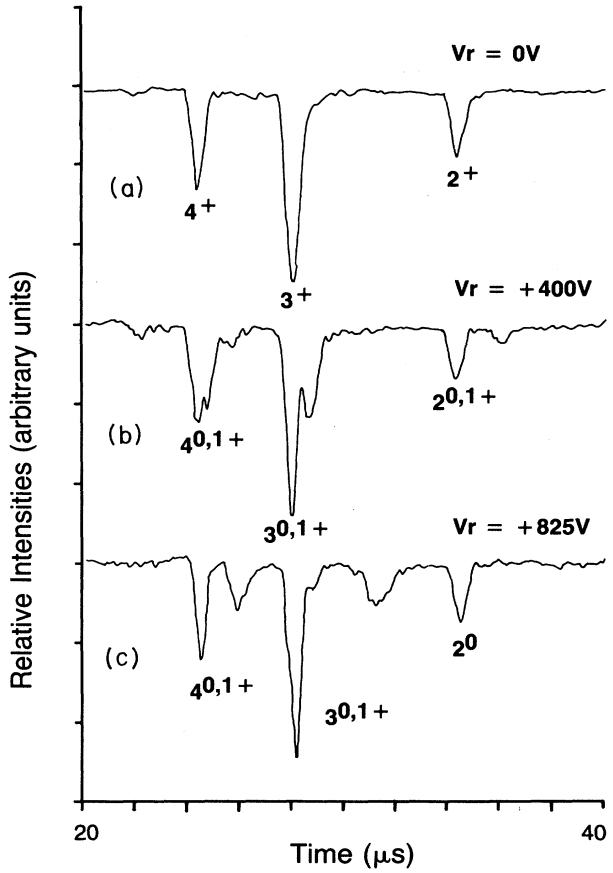

FIG. 2. TOF spectrograms of about 400-eV/charge aluminum 2+, 3+, and 4+ ions scattered from a gold surface at 7° grazing incidence and specularly reflected. (a) No retarding potential across the retarding gap (RG, Fig. 1). (b) A potential of +400 V across the gap. (c) A potential of +825 V across the gap.

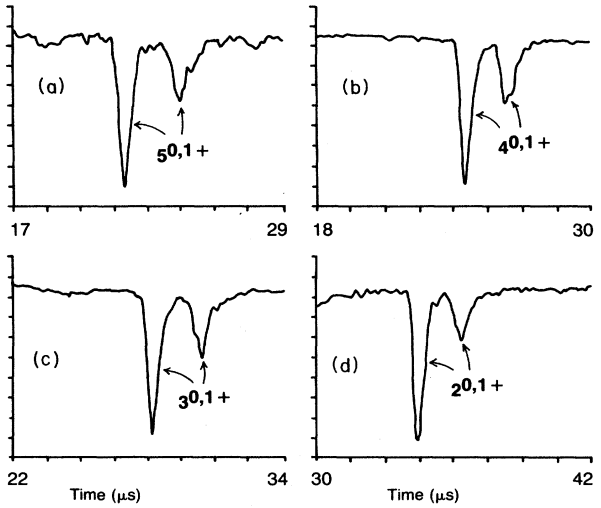

FIG. 3. Representative TOF spectrograms of gated aluminum ion packets scattered from a gold-iridium surface incident at 7° and specularly reflected. (a) 2000-eV 5+ ion packets with +1400 V across the retarding gap. (b) 1600-eV 4+ ion packets with +960 V across the gap. (c) 1200-eV 3^+ with 720 V across the gap. (d) 800-eV 2+ with +400 V across the gap.

from the gold-iridium target. Figure 4 shows the response of detector $C1$ when about 280-eV/charge carbon ions, incident at 7°, were specularly reflected. Spectrograms using carbon ions had the same appearance independent of the retarding potential, indicating no residual charge. The scattered carbon ions come off the surface fully neutralized within experimental error.

Attempts were made to find charge using the CEMA detector inside the chamber by applying positive potentials to the grids while keeping the angle of incidence at 7°. There was no evidence of residual charge left after scattering of the ions through angles of deviation equal to

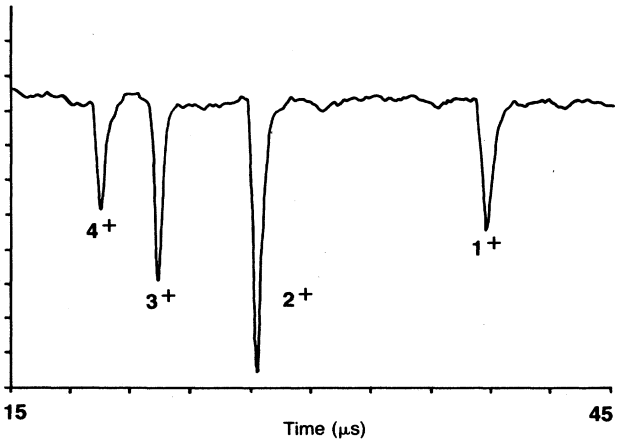

FIG. 4. TOF spectrogram of 280-eV/charge carbon ions scattered under the same conditions as Fig. 2(a). Spectrograms taken with retarding potentials applied to the retarding gap gave the same result, indicating no residual charge.

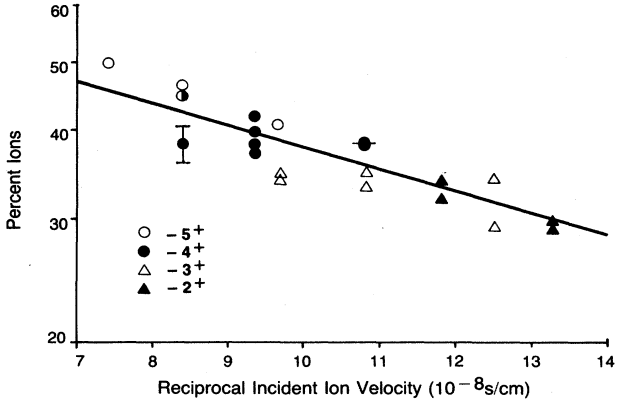

FIG. 5. Fraction of Al^+ ions remaining after multicharged aluminum ions incident at 7° to the target surface are specularly scattered vs the reciprocal of the incident ion velocity. The error bar on the 4+ point is meant to represent the reproducibility uncertainty.

or greater than 45°. Charge detection under these conditions is difficult, but the presence of appreciable charge should have been detected.

In an earlier experiment, attempts were made to detect residual charge using the sensitive long-arm TOF charge analysis on multicharged aluminum ions incident at 22.5° on a gold surface and specularly reflected.[5] No charge was detected.

Figure 5 shows a semilog plot of the fraction of Al^+ ions remaining in multicharged aluminum ion packets, incident at 7° and specularly reflected, versus the reciprocal velocity of the incident ion. The plot shows that Al^0 is the dominant species and becomes increasingly dominant as the *velocity* decreases.

DISCUSSION

It appears that the neutralization of *slow* multicharged ions on a metal surface does indeed follow a model where step-wise Auger neutralization takes place on the incoming pass. There appears to be no memory of the original charge state. Once the multicharged ions have fully interacted with the metal target on the incoming pass they seem to all possess the same charge character on the outgoing pass, which depends on the atomic species and velocity of the ion, but not on the incident charge state.

One can ask whether either the Al projectile or the C projectile begins its outgoing pass as a neutral or as a singly charged ion. For a slow collision with the metal target, it likely begins as an ion. Even if the kinetic energy of incident transverse motion is sufficient to guarantee penetration of the surface layer, these projectiles cannot exist as neutrals with bound states in the metal. The ionic nuclear charge is inbedded in a conducting medium. The ionic electric field is greatly weakened by the plasma shielding.[6] The shielding is characterized by the Debye screening length, $\lambda_D \approx 0.7$ Å calculated for gold. The Coulomb potential of the nuclear charge becomes a screened potential.[7] The electrons that are bound to the ionic charge move out to larger atomic orbits. Those

electrons that move to radial distances greater than the cutoff distance are no longer bound. The $3p$ electron in a normal neutral Al ($1s^2 2s^2 2p^6 3s^2 3p$) configuration has a binding energy of only 6.0 eV, and is surely unbound in the metal. For normal carbon in the C ($1s^2 2s^2 2p^2$) configuration, the $2p$ electron has a binding energy of 11.3 eV, and is likely unbound in the metal. In fact, C and Al are located near adjacent "Z_1" oscillations in stopping power measurements. These oscillations are postulated to be caused by scattering resonances in the electronic structure of the atoms in a metal.[8]

Figure 6 is a schematic diagram of energy levels, measured relative to the vacuum level, pertinent to the outgoing pass. The work function and Fermi level (F) is shown for gold as 5.1 eV with the bottom of the conduction band taken as 10.6 eV, measured from the vacuum level. Also shown is the top of the filled core $5d^{10}$ band for gold at about 7.6 eV. The binding energies of ground-state Al^0 (G) and C^0 (G) atoms are shown far removed ($S=\infty$) from the surface where S is the distance from the surface measured in Å. Plotted is $E(S)=E_\infty-3.6/S$, where E_∞ is the energy at $S=\infty$ and $3.6/S$ is the image energy in eV and S is measured in Å. (The meaning of S is clouded, of course, when S becomes comparable to atomic dimensions.) The atomic energy levels are drawn by aligning the ground state of the appropriate ionization state with the vacuum level. (It would seem reasonable that the target surface would be more goldlike since diffusion of iridium into the gold occurs primarily at the backside interface. Even if the diffusion were complete, the picture developed in Fig. 6 would probably not be too far in error for our purposes since Au and Ir are both classed as metals and have atomic numbers of 79 and 77, respectively, and work functions of 5.1 and 5.27 eV, respectively. The charge fractions quoted here are similar to those rough results quoted in Ref. 1 which represented scattering from a gold target.)

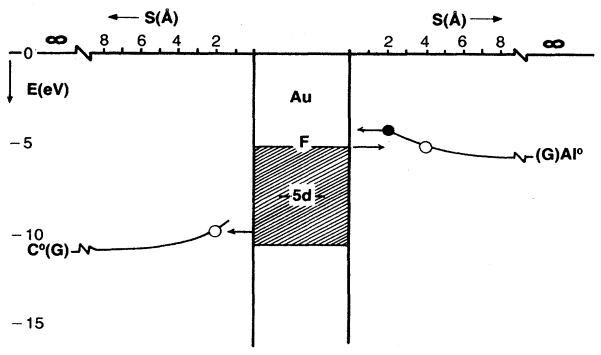

FIG. 6. Plot of pertinent energy levels in carbon and aluminum ions receding from a gold surface. The solid lines labeled with G represent the ground state of the projectile atom vs distance from the surface—carbon on the left and aluminum on the right. F represents the Fermi level and $5d$ represents the top of filled $5d$ band in gold (see text).

A simple picture would be that an Al^+ emerges from the surface with a vacancy in the $3p$ orbital. Once outside the surface the $3p$ orbital is in resonance with the open metal electron states above the Fermi level F. This insures that the aluminum projectile starts from the surface as an Al^+ ion. As it recedes from the surface, the image energy is reduced to the point where the $3p$ vacancy is in resonance with the top of the conduction band. Since the ionization energy for a free neutral atom is only 0.9 eV greater in magnitude than the work function of gold, resonance would occur at $S=4$ Å. At this point resonance ionization is still possible. Beyond this point ($S>4$ Å) only resonance neutralization is possible since an electron that is captured by the ion cannot get back to the metal. This option is blocked by the Pauli principle. The capture process then becomes one-way neutralization. If the ion passage from the surface to infinity is done slowly (adiabatically), then one expects 100% neutral from the scattering process.

Again using the simple picture described in Fig. 6, one notes that the ionization energy of C^0 (G), E_∞, is only 0.7 eV greater in magnitude than the energy at the bottom of the band (also a near resonance), but is 6.4 eV from the Fermi level, F. If carbon projectile emerges as C^+ from the gold, one-way resonance neutralization takes place, immediately filling the $2p$ vacancy. Thus, again neutrals are expected.

The picture drawn in Fig. 6 does not fully describe the charge exchange process. The resulting charge state at infinity also depends on the atomic ground-state broadening at distances near the surface which is caused by the atomic interaction with the electronic states in the metal. This broadening is a function of the distance from the surface.[9-11]

The ideas of adiabatic and nonadiabatic behavior in this problem can be easily visualized from the concept originally attributed to Massey and extensively used by Hasted[12] in the analysis of charge exchange in atomic collisions. The characteristic electron transition time associated with such a collision is given by $t_r^{-1}\sim\Delta E/h$, where ΔE is the energy defect of the reaction, $\Delta E\sim|E_a-F|$ in our case where E_a is an atomic energy level. Here the actual collision time is $t_c=a/v_z$, where a is the characteristic interaction distance and v_z is the velocity of recession perpendicular to the surface. The collision is considered adiabatic if $t_c\gg t_r$. Thus $\langle\Delta Ea\rangle/hv_z\gg1$ would be the rough criterion for adiabatic behavior. Reference 10 makes a careful analysis of a problem similar to our present problem which suggests that $R=A\exp(-v_0/v_z)$, where R is the relative number of scattered particles having a charge state not expected from adiabatic behavior. (Truly adiabatic behavior should give $R=0$.) The quantities A and v_0 are dependent on the atomic level broadening. The fraction R then is a measure of the nonadiabatic behavior. Figure 5 can be converted to a plot of R versus v_z^{-1} by dividing the values on the abscissa by sin7°. The line through the data is $R=0.8\exp(-8.7\times10^5/v_z)$, where v_z is measured in cm/s.

Reference 10 contains an analysis of the scattering of "hyperthermal" Na atoms from a W surface.[13] The

problem presented here is very similar in that near resonance exists in both cases between E_∞ and F. The difference is that in our problem the atomic level actually crosses F without considering atomic broadening (Fig. 6), while in the Na case the atomic level remains above F insuring a majority species of Na^+. (The authors of Ref. 10 could not compare their calculations with the experimental results of Ref. 13 since absolute values of R were not determined, unlike our results.) If we simply interpret $v_0 = \langle \Delta Ea \rangle / h$, then $\langle \Delta Ea \rangle = 0.36$ eV Å. The interaction distance a must be near a surface distance of a few Å (atomic dimensions). This suggests that $\Delta E \sim 0.1$ eV. Thus the simple picture expressed in Fig. 6 is indeed at least qualitatively correct. Nonadiabatic neutralization is dominated by a narrow resonance crossing.

A more reasonable way to analyze the results displayed in Fig. 5 is to use the theoretical interpretation especially developed for ions on surfaces, such as described by Brako and Newns,[10] then $v_0 = 2\Delta_0 a = 4.0 \times 10^{-3}$ a.u. (atomic units), where Δ_0 is the width of the atomic ground state around resonance with the Fermi level and a is the range of the interaction. If we let $a \sim 7$ a.u., then $\Delta_0 \sim 3 \times 10^{-4}$ a.u. $\sim 8 \times 10^{-3}$ eV, which is physically close to kT at room temperature.

One expects that specular reflection at grazing incidence should represent the most adiabatic of the scattering conditions for a given electrostatic analyzer setting. It is also true that penetration of the surface at grazing incidence and specular reflection is minimal. The data points displayed in Fig. 5 represent analyzer settings corresponding to about $E_0 = 500$, 400, 300 eV/charge. The kinetic energy of transverse motion to the surface thus corresponds to $E_z = 7.4$, 5.9, and 4.5 eV/charge, respectively, where $E_z = E_0 \sin^2 7°$. The highest transverse kinetic energy in Fig. 5 is thus about 37 eV and the lowest is 9.0 eV. This portion of the experiment involves small transverse energies where surface penetration is expected to be small. A 1600-eV Al ion has a transverse energy of about 24 eV at our angle. Using the arguments of Snowdon *et al.*,[14] these projectiles can be calculated to approach no closer than about 3 Å to the atomic surface plane treating our amorphous surface as a crystalline surface. Oen and Robison[15] have calculated that 75% of 1-keV H atoms penetrate no deeper than 3.6 Å into an *amorphous* Cu surface when scattered at an angle of incidence of 19° to the surface.

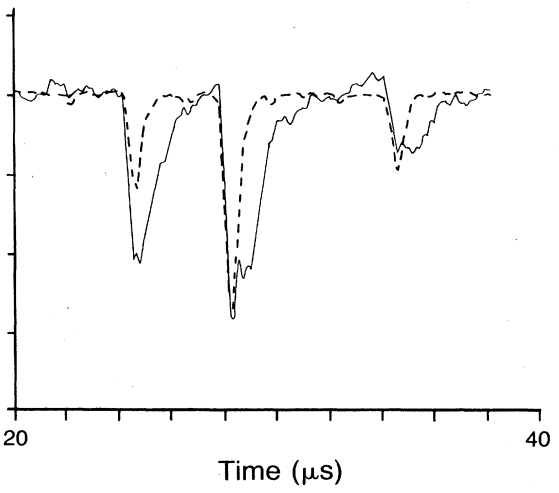

FIG. 7. A TOF spectrogram of Al ions specularly scattered from a smooth metal target at 7° incidence is superimposed on a spectrogram taken under the same conditions after Ar-ion etching of the surface. (Dashed line, before etching with no retarding field; solid line, after etching with/without retarding field).

The importance of a smooth polished surface in these results was demonstrated by the following experiment. The thick-film surface of the target was subsequently subjected to a mild discharge of 3-keV Ar ions that noticeably ion etched the surface. The Al ion scattering from this slightly roughened, unannealed surface at grazing incidence was much different. Little evidence of charge remained after scattering. Also the aluminum line widths were much broader, as seen in Fig. 7. The increased linewidth is indicative of elastic and inelastic energy losses typical of bulk interaction with the target complete with multiple scattering.

CONCLUSIONS

It appears that nonadiabatic (Al^+ survival) behavior in this experiment with aluminum ions at these velocities requires little intimate contact with the bulk of the metal. The structureless surface picture shown in Fig. 6 seems valid only for minimal interaction with the surface provided by low-velocity ions incident at a grazing angle on a smooth surface. We note that total neutralization results from the specular reflection of aluminum ions incident at 22.5° to the surface of a smooth gold target. We also note that neutralization is heavy when the ions are incident at grazing incidence to the surface of a smooth metal surface, but are scattered at larger angles of deviation. Neutralization is also heavy when the surface is roughened by ion etching, even for specular reflection at grazing incidence.

A common characteristic in all our experiments that produce heavy neutralization is a heavy energy loss of the scattered projectiles, not unlike that shown in Fig. 7 for a roughened surface, which shows a bulk interaction. The heavy neutralization anomalies in the present Al ion experiment, relative to specular scattering from a smooth surface at grazing incidence, appear to be related to penetration of the surface with subsequent electronic and atomic collisions in the bulk. The violent high-frequency collisions, when the projectile interacts with the bulk, produces local metal electronic excitation as well as projectile atomic excitation. Using the arguments of Fermi and Teller,[16] the mean energy loss of a heavy projectile in collision with an electron near the top of the conduction band is about $\Delta E = mVv_f$, where m is the electronic mass, V is projectile speed ($\sim 10^7$cm/s), and v_f is the metal Fermi velocity ($\sim 10^8$ cm/s). This is about 0.6 eV, which is the excitation energy given to the conduction electron, placing it in an excited state above the Fermi level, making it available for capture. However, this electronic energy should be rapidly dissipated among the oth-

er electrons at the top of the conduction band[17] which minimizes the effect despite the large number of electrons that are excited. (Using the work of Arnau *et al.*,[18] the stopping power for Al in an electron gas is about 2 eV/Å at our velocities, and assuming a one-electron radius for gold[19] to be 1.5. It has also been demonstrated that electron promotion through curve crossings in close atomic encounters in a solid can be important in electronic excitation.[20])

Excitation of the projectile by the atom-atom rearrangement collisions in the bulk at these collisional energies can play a role. The shielding of the conduction electrons reduces the effective excitation energies and increases the size of the orbital radii such that the projectile atom may not emerge as a normal atom. The additional excitation energy may make the resonance neutralization picture not entirely realistic with nonresonance Auger neutralization processes coming into play. The violent, high-frequency multiple collisions in the bulk also broadens the initial atomic level width as it emerges from the surface, which then decays as the projectile recedes from the surface.

SUMMARY

A considerable fraction (40%) of multicharged Al ions with incident kinetic energies of a few hundred eV/charge remain as singly charged ions after being specularly scattered from a smooth metal (gold-iridium) surface. Any experimental condition that produces appreciable intimate contact with the target bulk destroys the ionic content of the partially neutralized scattered projectiles. In this respect the experiments of Akazawa and Murata[21] are interesting since they also find penetration depth important. In the case of specular scattering at grazing incidence from a smooth metal surface, the ionic residual can be analyzed as the nonadiabatic fraction $R = A \exp(-v_0/v_z)$ as suggested in Ref. 10.

ACKNOWLEDGMENTS

The research described here was supported by the National Science Foundation through Grant No. DMR-85-76109, jointly funded by the Atomic, Molecular, and Plasma Physics Program and the Solid State Physics Program.

---

*Present address: Department of Physics, Peking University, Beijing 100 871, People's Republic of China.

[1]R. H. Hughes, D. O. Pederson, and X. M. Ye, Appl. Phys. Lett. **47**, 1282 (1985).

[2]H. D. Hagstrum, Phys. Rev. **96**, 325 (1954); V. A. Arifov, L. M. Kishinevski, E. S. Mukhamadiev, and E. S. Parilis, Zh. Tekh. Fiz. **43**, 181 (1973) [Sov. Phys. Tech. Phys. **18**, 118 (1973)].

[3]L. G. Gray, R. H. Hughes, and R. J. Anderson, J. Appl. Phys. **53**, 6628 (1982); R. H. Hughes, R. J. Anderson, C. K. Manka, M. R. Carruth, L. G. Gray, and J. P. Rosenfeld, *ibid.* **51**, 4088 (1980).

[4]R. H. Hughes, G. Wattuhewa, R. D. Miller, X. M. Ye, and D. O. Pederson, Phys. Rev. B **36**, 9003 (1987).

[5]X. M. Ye, doctoral dissertation, University of Arkansas, 1986 (unpublished).

[6]D. Pines and D. Bohm, Phys. Rev. **85**, 338 (1952).

[7]T. L. Ferrell and R. H. Ritchie, Phys. Rev. B **16**, 115 (1977).

[8]P. M. Enchenique, R. M. Nieminen, J. C. Ashley, and R. H. Ritchie, Phys. Rev. A **33**, 897 (1986).

[9]A. Blandin, A. Nourtier, and D. W. Hone, J. Phys. (Paris) **37**, 369 (1976); W. Bloss and D. Hone, Surf. Sci. **72**, 277 (1978).

[10]R. Brako and D. M. Newns, Surf. Sci. **108**, 253 (1981).

[11]W. Bloss and D. Hone, Surf. Sci. **72**, 277 (1978).

[12]J. B. Hasted, *Physics of Atomic Collisions* (Butterworth, Washington, D.C., 1964), Chap. 12.

[13]E. G. Overbosch, B. Rasser, A. D. Tenner, and J. Los, Surf. Sci. **92**, 310 (1980).

[14]K. J. Snowdon, D. J. O'Connor, and R. J. MacDonald, Phys. Rev. Lett. **61**, 1760 (1988).

[15]O. S. Oen and M. T. Robinson, Nucl. Instrum. Methods **132**, 647 (1976).

[16]E. Fermi and E. Teller, Phys. Rev. **72**, 399 (1947).

[17]P. A. Wolff, Phys. Rev. **95**, 56 (1954).

[18]A. Arnau, P. M. Echenique, and R. H. Ritchie, Nucl. Instrum. Methods Phys. Res. B **33**, 138 (1988).

[19]A. Mann and W. Brandt, Phys. Rev. B **24**, 4999 (1981).

[20]G. Falcone and Z. Sroubeck, Phys. Rev. B **38**, 4989 (1988).

[21]H. Akazawa and Y. Murata, Phys. Rev. Lett. **61**, 1218 (1988).